Preprints of the 19th World Congress
The International Federation of Automatic Control
Cape Town, South Africa. August 24-29, 2014

Funnel control for oxygenation during artificial ventilation therapy

Anake Pomprapa*, Sergio R. Alfocea*, **, Christof Göbel*,**
Berno J. E. Misgeld* and Steffen Leonhardt*

** Philips Chair for Medical Information Technology,*
RWTH Aachen University, Aachen, Germany,
(e-mail: pomprapa@hia.rwth-aachen.de)
*** Escola Tècnica Superior d'Enginyeria de Telecomunicació de Barcelona - UPC, Barcelona, Spain*
**** Weinmann Geräte für Medizin GmbH, Hamburg, Germany*

Abstract: A patient with hypoxia requires immediate oxygen therapy to enhance oxygenation. Individual model including disease and parameter variation is needed, which limits all model-based approaches for the task of reference tracking control. In this article, a non-identifier based control algorithm, called funnel control, is proposed to solve this clinical problem in real practice. With this control technique, it requires less a priori knowledge of the complicated nonlinear and time-delay plant. The design of a funnel controller relies only upon an output feedback and the difficult control problem of such system is simplified by the design of a funnel boundary, which is a time-varying gain to force error dynamics inside this boundary. Funnel controllers with relative degree one and two are presented and simulated with the proposed cardiopulmonary system for low tidal volume, simulating the existing and abrupt change of atelectasis.

Keywords: funnel control, mathematical model of cardiopulmonary system, oxygenation, closed-loop control, oxygen therapy, biomedical control systems.

1. INTRODUCTION

In respiratory care, oxygenation is one of the most important parameter during ventilation therapy because oxygen (O_2) is necessary for cell metabolism and tissues. For instance, heart or brain requires sufficient oxygen to maintain their functions. Thereby, severe hypoxia or a condition in which oxygen levels in arterial blood are low should be avoided in clinical practice, otherwise the result may be multiple organ failure and mortality (Zambon and Vincent, 2008). Typically, oxygen therapy is required to recover the critical situation by increasing the fraction of inspired oxygen concentration (FiO_2) for the subject (Claure and Bancalari, 2013), which is considered as a control input in this context. To assess oxygenation, arterial oxygen tension (PaO_2) and arterial oxygen saturation (SaO_2) are two possible parameters (Pierson, 2013). However, SaO_2 is chosen to be a controlled variable because of its availability to be continuously measured in real time, while PaO_2 can only be measured by blood gas analysis (BGA), which can be done only by blood samples and is limited by total allowable amount of blood samples to be taken. In this article, the automatic control design algorithm to manage hypoxia is based on a single-input single-output (SISO) system for ventilation system using oxygen therapy.

To facilitate the controller design for this particular application, a mathematical model of the complex cardiopulmonary system is required, in order to represent the hypoxia behaviour of the human system and to evaluate the control performance. The selected model (Fincham and Tehrani, 1983a,b) expresses gas exchange, gas transport and gas storage system using differential equations based on mass balance principles. The dynamic characteristics of the system include transient and steady state solution of O_2 and CO_2. However, only the model for O_2 is of concern in context of this paper. Due to oxygen therapy, O_2 will be supplied to a critically ill patient by a mechanical ventilator with adjustable FiO_2. The simulated cardiopulmonary model is based on the periodic breathing applied to the lung compartment and gas is transported by the circulating blood to other compartments, for example brain and body including transport delay. This model will be used to simulate patient dynamics under hypoxia. The aim of this work is to design a funnel controller to recover the critical situation using oxygen ventilation therapy and it should be optimized the oxygen supply in order to avoid O_2 toxicity that may be triggered (Clark, 1974).

Funnel control is a non-identifier-based adaptive control with no requirement of an identification mechanism for the plant model, proposed in 2002 (Ilchmann *et al*., 2002). The exact knowledge of the system parameters is not required (Mandaloju and Trenn, 2006). The control objective is to asymptotically regulate the output of the system, which is the oxygenation measured by SaO_2 in this context and small output error is often allowed (Bullinger and Allgöwer, 2005). This control algorithm also guarantees transient performance, so that the evolution of the tracking error should be within a prescribed performance funnel (Ilchmann *et al*., 2004). Funnel control is applicable to a system with relative degree one and two (Hackl *et al*., 2013), stable zero dynamics and positive high-frequency gain. All states of the closed-loop system are bound by the output regulation using the funnel controller (Ilchmann and Mueller, 2009a). The control scheme has been successfully implemented in various applications, for instance speed and position control of a rotary system with unknown friction and load disturbances

(Hackl *et al*., 2011). In our medical application, additional oxygen molecules given to the subject usually bind to haemoglobin that lacks of oxygen molecule. An increase in oxygen concentration leads to an increase in SaO_2. The nature of this system is globally minimum phase and has stable zero dynamics. Thus, funnel control is suitable for this application.

This contribution is organized as follows. It begins with the mathematical model describing oxygen dynamics in section 2 to provide the background for this particular system and the simulation result for hypoxia, followed by a design of funnel control for this critical situation in section 3. Simulation results for the evaluation of control performance and a discussion are given in section 4 and 5, respectively. The article ends with the conclusion in section 6.

2. SYSTEM MODELLING

2.1 Modelling of the cardiopulmonary system

The development of mathematical models for the cardiopulmonary system has a long history and dates back to the 1960 (Defares *et al*., 1960). The selected and optimized model structure for a human undergoing hypoxia, shown in Fig. 1, is based on a three-compartment model consisting of lungs, brain and lumped body tissue (Fincham and Tehrani, 1983a). The system additionally comprises a cardiac output controller and a brain blood flow controller to identify the cardiac flow (Q_C) and the brain blood flow (Q_B), respectively.

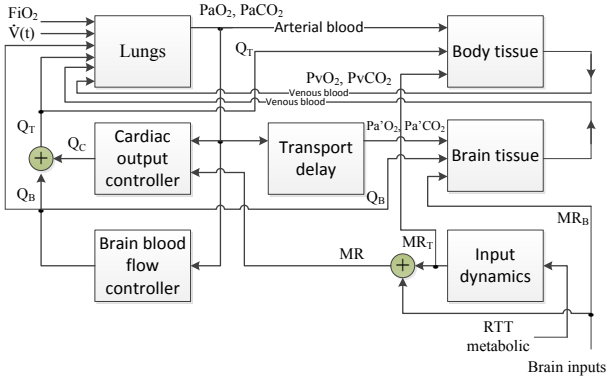

Fig. 1. Block diagram of the cardiopulmonary system using three-compartment model.

Lung compartment

Based on mass balance equation of eq. (1), $C_{VT}O_2$, $C_{VB}O_2$ and C_aO_2 denote oxygen volume concentration of venous body tissue compartment, of venous brain compartment and of arterial vessel with the unit of l(STPD)/l, respectively. Q_T is total blood flow (l/s), which is a combination of Q_B and Q_C. $V(t)$ expresses the dynamics of tidal volume in litre (l). P_AO_2 represents alveolar O_2 tension (mmHg). $P_b - 47$ is the barometric pressure minus water vapour pressure at body temperature (mmHg).

$$\frac{dP_AO_2}{dt} = \frac{P_b - 47}{V(t)} \cdot [K1 - (C_{VT}O_2 - C_aO_2)Q_T - (C_{VB}O_2 - C_aO_2)Q_B] \quad (1)$$

for inspiration ($\frac{dV(t)}{dt} \geq 0$), $K1 = \frac{(P_iO_2 - P_AO_2)}{P_b - 47} \cdot \frac{dV(t)}{dt}$

and for expiration ($\frac{dV(t)}{dt} < 0$), $K1 = 0$,

The assumption for alveolar O_2 tension (P_AO_2) is made based on $P_AO_2 = P_aO_2 + 4$ in mmHg representing a relationship of blood-gas interface, where P_aO_2 represents arterial O_2 tension and P_iO_2 is inspired oxygen tension.

Therefore, the value of P_aO_2 can be evaluated at any particular time of breathing. To compute O_2 tension at any points of measurement, the blood gas relationship is used to convert volume concentration of O_2 in the blood (C_{O_2}) [l(STPD)/l] to O_2 tension (PO_2), provided in eq. (2).

$$C_{O_2} = 0.2 \cdot (1 - e^{-0.046 \cdot PO_2})^2 \quad (2)$$

Subsequently, arterial oxygen saturation (S_aO_2) can be estimated by the relationship providing in eq. (3) (Fincham and Tehrani, 1983b), while S_aO_2 has a unit in percent (%).

$$S_aO_2 = (1 - e^{-0.046 \times PaO_2})^2 \times 100\% \quad (3)$$

This relationship contributes to nonlinear behavior of the cardiopulmonary system for the control output S_aO_2.

Lumped body tissue compartment

A mass balance eq. (4) describes the mathematical relationship of oxygen concentration at the body tissue compartment.

$$\frac{dC_TO_2}{dt} = -\frac{1}{S_T}[(C_{VT}O_2 - C_aO_2) \cdot Q_T + MR_TO_2], \quad (4)$$

where MR_TO_2, S_T and C_TO_2 denote metabolic rate in body tissue for O_2 (0.00352 l/s), equivalent gas storage space at tissue (50 l) and O_2 volume concentration at body tissue.

Brain tissue compartment

Similarly, eq. (5) expresses the relationship of oxygen concentration at the brain tissue compartment.

$$\frac{dC_BO_2}{dt} = -\frac{1}{S_B}[(C_{VB}O_2 - C'_aO_2) \cdot Q_B + MR_BO_2], \quad (5)$$

where C'_aO_2, MR_BO_2, S_B and C_BO_2 represent volume concentration of O_2 in the arterial blood with a time-delay, metabolic rate in brain for O_2 (0.000925 l/s), equivalent gas storage space at brain (1.1 l) and O_2 volume concentration at brain, respectively.

Input dynamics

An increase in the level of exercise can be simulated by adapting a step change at the RTT metabolic input, standing for the magnitude of the step defining the final value of MR_T. The tissue metabolism MR_T is shaped by eq. (6).

$$\frac{d(MR_T)}{dt} = \frac{RTT - MR_T}{\tau}, \quad (6)$$

where τ denotes exercise metabolism dynamic (30 s). Brain input or brain tissue metabolism (MR_B) is assumed to be constant for O_2 (0.000925 l/s) and RTT is the magnitude of the step denoting the final value of MR_T. Therefore, the total body metabolism MR can be expressed by the sum of tissue

and brain metabolism.

$$MR = MR_T + MR_B \quad (7)$$

Eq. (7) is used to define the metabolic rate ratio MRR.

$$MRR = \frac{MR}{basal\ level\ of\ MR}, \quad (8)$$

where basal O_2 level of MR = 0.004445 l/s.

Transport delay

Arterial blood gas tension is assumed to be delayed by 10 s at the brain tissue (Fincham and Tehrani, 1983a). $P_a'O_2$ and $P_a'CO_2$ symbolize arterial gas tension with time delay for the brain compartment.

Cardiac output controller

Fincham and Tehrani (1983b) modelled cardiac flow by the algebraic sum of Chebyshev polynomials ($T_j(\bar{X}_i)$) of the first kind of degree j in terms of PaO_2, $PaCO_2$ and metabolic rate ratio MRR.

$$Q_C = E[Q_C] + Q_{C1} + Q_{C2} + Q_{C3}, \quad (9)$$

where $E[Q_C]$ = 0.08333 l/s. The details of how to compute Q_{Ci} ($i \in \{1,2,3\}$) are given in Fincham and Tehrani, 1983b. For instance, Q_{C1} can be computed as

$$Q_{C1} = \begin{cases} 10^{-5} \cdot \sum_{j=0}^{5} A_j T_j(\bar{X}_i) & ,for\ 25 \le PaO_2 < 95, \\ 0 & ,for\ \ PaO_2 \ge 95, \end{cases} \quad (10)$$

where A_0 = 2445.1, A_1 = -3233.3, A_2 = 1050.4, A_3 = -143.5, $A_4 = A_5 = 0$, $\overline{X_1} = \frac{2PaO_2 - 115}{65}$ and chebyshev polynomials

$T_0(x) = 1$, $T_1(x) = x$, $T_2(x) = 2x^2 - 1$, $T_3(x) = 4x^3 - 3x$, $T_4(x) = 8x^4 - 8x^2 + 1$ and $T_5(x) = 16x^5 - 20x^3 + 5x$.

Similarly, Q_{C2} and Q_{C3} can be calculated by different definitions of A_j, $\overline{X_2}$ and $\overline{X_3}$.

Brain blood flow controller

Similar to the cardiac flow, brain blood flow can be expressed with the algebraic sum of Chebyshev polynomials ($T_j(\bar{X}_i)$) in terms of PaO_2 and $PaCO_2$.

$$Q_B = E[Q_B] + Q_{B1} + Q_{B2} + Q_{B3}, \quad (11)$$

where $E[Q_B]$ = 0.0125 l/s. The details for a computation of Q_{Bi} ($i \in \{1,2,3\}$) are listed in Fincham and Tehrani, 1983b.

2.2 Simulation results of the cardiopulmonary model

The dynamics of oxygenation consist of a fourth-order non-linear model with transport delay. The transient response of hypoxia was simulated by a step input changing from 21% to 9% oxygen breathing between 20 and 40 min and air breathing (21%) for other simulation time with the results given in Fig. 2.

A normal tidal volume of 0.25 l with a functional residual capacity of 2.2 l, inspiratory to expiratory ratio (I:E) of 1:1, respiratory rate of 15 bpm and CO_2 in the air for 0.0387% were set for this simulation. Once the system is introduced by FiO_2 = 0.09 or 9%, the response is under hypoxia condition. PaO_2 and SaO_2 fall rapidly within 100 s. When hypoxia prolongs for 20 min, PaO_2 and SaO_2 continuously decrease to a severe condition of SaO_2 = 60%. After re-exposure to air of 21% of oxygen concentration for 20 min, oxygenation returns to its normal value.

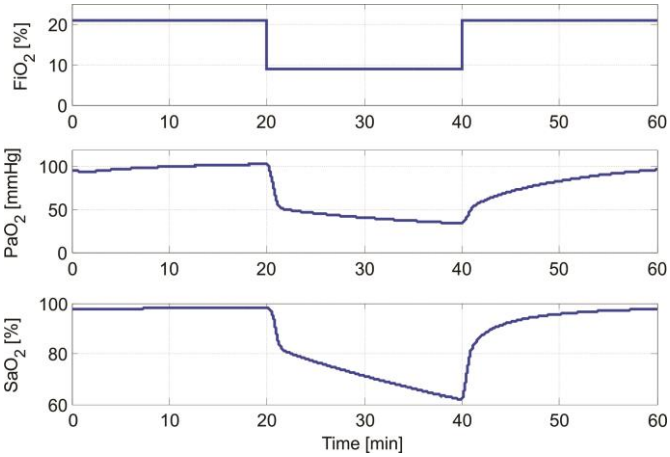

Fig. 2. Hypoxia response of the cardiopulmonary system with FiO_2 = 9% during time between 20 and 40 min.

Next, a clinical scenario for atelectasis or loss of lung volume was simulated by introducing only one lung ventilation (a tidal volume of 0.125 l) and the result of simulation is shown in Fig. 3. For time < 20 min, PaO_2 and SaO_2 gradually decrease and poor oxygenation can be observed, even though FiO_2 is set at 21%. During the time in between 20 and 40 min, FiO_2 is increased to 100%, 75% and 50% of different operating points in order to compare the responses. Improved oxygenation for both PaO_2 and SaO_2 can be achieved with different dynamics.

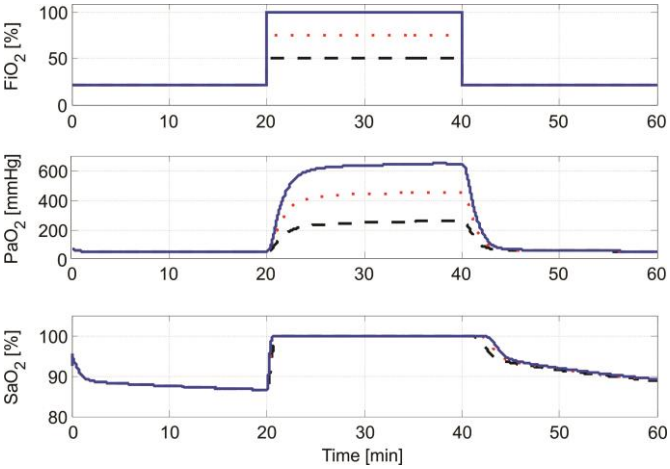

Fig. 3. Hypoxia response due to tidal volume of 0.125 l using oxygen therapy for FiO_2 = 100%, 75% and 50% during time between 20 and 40 min.

After the time > 40 min, fresh air of FiO_2 = 21% is exposed to the model of atelectasis with low tidal volume (0.125 l).

The system is under hypoxia condition again. Therefore, this model is suitable for further design of funnel controller with the objective to control SaO_2. The control input FiO_2 shall be used to regulate the controlled output of SaO_2, which is regarded as a single-input single-output (SISO) system with nonlinear and time-delay and this therapeutic approach is called "oxygen therapy".

3. CONTROL SYSTEM DESIGN

3.1 Funnel control design with relative degree one

Funnel control is applicable to a wide class of systems described by functional differential equations (Ilchmann and Mueller, 2009b). A design of a funnel control system requires less a priori knowledge of the complicated plant with various possible properties including infinite-dimensional, nonlinear, time delay, hysteresis or chaotic behaviour (Ilchmann *et al*., 2002). To implement the control of oxygenation, a control structure of funnel control system is provided in Fig. 4.

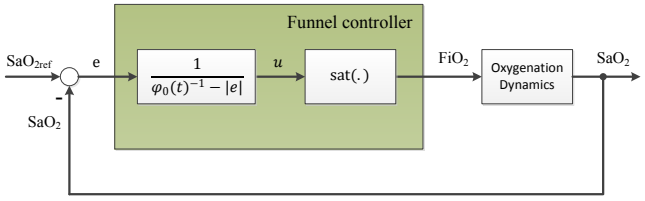

Fig. 4. Block diagram of funnel controller of relative degree one with saturation for oxygenation dynamics.

FiO_2 is generated by a saturation limitation

$$FiO_2(t) = sat(u(t)) \,, \tag{12}$$

where $sat(u) = \begin{cases} 0.21 & for\ u \le 0.21 \\ u & for\ 0.21 \le u \le 1 \\ 1 & for\ u > 1 \end{cases}$ in order to cope with a limitation for the fraction of inspired oxygen concentration (FiO_2) in between 0.21 and 1 or from fresh air (21%) to pure oxygen of 100 %. The controlled signal computed from the funnel controller with relative degree of one is given as follows.

$$\mathrm{u(t)} = \mathrm{k_0(t)} \cdot \mathrm{e(t)} \,, \tag{13}$$

where $\mathrm{e(t)} = \mathrm{SaO_{2ref}} - \mathrm{SaO_2}$ and $\mathrm{k_0(t)} = \frac{1}{\varphi_0(t)^{-1} - |\mathrm{e}|}$, which is a time-varying non-monotonic gain.

The funnel boundaries ($\mathrm{F_{\varphi_0}(t)} = \varphi_0(t)^{-1}$) restricts the error to evolve inside the funnel boundary given in a set of $\{(t,e) \in R_{\geq 0} \times R : |e| < \varphi_0(t)^{-1}\}$. High feedback gain is required whenever $|e|$ is close to the funnel boundaries $\mathrm{F_{\varphi_0}(t)}$. The inverse of vertical distances of $\varphi_0(t)^{-1} - |e|$ is used to compute the gain $\mathrm{k_0(t)}$.

To design the funnel boundary for $\mathrm{e(t)}$, $\varphi_0(t)$ is defined as $\varphi_0(t) = \frac{0.6 \cdot t}{1.2 \cdot t + 100}$, such that the initial $\mathrm{e(0)}$ is within 100 and $\lambda_0 = \lim_{t \to \infty} \varphi_0(t)^{-1} = 2$, which determines the upper bound of the funnel boundary at $\mathrm{t} \to \infty$. The dynamical response can be designed by the change of coefficients in $\varphi_0(t)$. The tracking error is ultimately bounded by λ_0. There are a number of options to design the funnel boundary. For instance, the funnel boundary in the form of exponential function (Hackl *et al*., 2007) can be defined with $\varphi_0(t)^{-1} = 98 \cdot e^{\left(-\frac{t}{30}\right)} + 2$, so that the initial $\mathrm{e(0)}$ is within 100 and $\lambda_0 = \lim_{t \to \infty} \varphi_0(t)^{-1} = 2$ similar to the hyperbolic function. The evaluation of these two different nonlinear boundary will be given in the next section for the simulation result of funnel controller with relative degree one.

3.2 Funnel control design with relative degree two

The extension of funnel controller for relative degree two was recently presented by Hackl *et al*., 2013. The block diagram of a funnel controller with relative degree two is shown in Fig. 5. Eq. (12) is also applied for this control configuration.

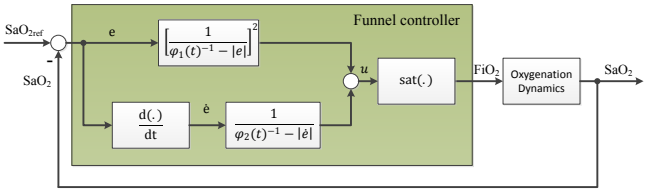

Fig. 5. Block diagram of funnel controller of relative degree two with saturation for oxygenation dynamics.

The controlled signal computed from the funnel controller with relative degree of two is given in eq. (14).

$$\mathrm{u(t)} = \mathrm{k_1(t)} \cdot \mathrm{e(t)} + \mathrm{k_2(t)} \cdot \dot{\mathrm{e}}(\mathrm{t}) \,, \tag{14}$$

where $\mathrm{k_1(t)} = \left[\frac{1}{\varphi_1(t)^{-1} - |e|}\right]^2$, and $\mathrm{k_2(t)} = \frac{1}{\varphi_2(t)^{-1} - |\dot{e}|}$. These non-monotonic gains are time-varying..

The control algorithm is based on output feedback and all signals are guaranteed to be bounded with a number of prerequisites (Ilchmann *et al*., 2002; Hackl *et al*., 2013):

(i) a system with relative degree two

(ii) stable zero dynamics or minimum phase

(iii) positive high-frequency gain.

The funnel boundaries ($\mathrm{F_{\varphi_1}(t)} = \varphi_1(t)^{-1}$ and $\mathrm{F_{\varphi_2}(t)} = \varphi_2(t)^{-1}$) restricts $\mathrm{e(t)}$ and $\dot{\mathrm{e}}(\mathrm{t})$ to evolve inside the funnel. High feedback gains are required whenever $|e|$ or $|\dot{e}|$ are close to the funnel boundaries $\mathrm{F_{\varphi_1}(t)}$ and $\mathrm{F_{\varphi_2}(t)}$, respectively. The inverse of vertical distances of $(\varphi_1(t)^{-1} - |e|)^2$ and $(\varphi_2(t)^{-1} - |\dot{e}|)$ are therefore used to compute the time-varying gains $\mathrm{k_1(t)}$ and $\mathrm{k_2(t)}$. With this approach, more aggressive gains can be assigned to system if $\mathrm{e(t)}$ and $\dot{\mathrm{e}}(\mathrm{t})$ get close to the boundaries.

The control of the cardiopulmonary dynamics under hypoxia can be achieved by the simple design of funnel boundaries with no need for the precise model of individual patient. It will ensure that $\mathrm{e(t)}$ and $\dot{\mathrm{e}}(\mathrm{t})$ lie within the prescribed funnel radii. However, a perfect reference tracking cannot be satisfied by using this control strategy. For the control of oxygenation, the goal is to keep SaO_2 in a clinical acceptable range of oxygenation, for example SaO_2 > 95%, with an optimal supply of oxygen to avoid oxygen toxicity.

To design the funnel boundaries for $\mathrm{e(t)}$ and $\dot{\mathrm{e}}(\mathrm{t})$, the initial errors have to lie inside the funnel boundaries. Therefore,

$\varphi_1(t) = \frac{0.6 \cdot t}{1.2 \cdot t + 100}$ is defined similar to the case of relative degree one. Additionally, $\varphi_2(t) = \frac{t}{0.01 \cdot t + 1.5}$ determines that the initial $\dot{e}(0)$ lies inside 1.5 and $\lambda_2 = \lim_{t \to \infty} \varphi_2(t)^{-1} = 0.01$. The dynamical response can be designed by the change of coefficients in $\varphi_1(t)$ and $\varphi_2(t)$. The tracking error and its error derivative are ultimately bounded by $\lambda_1 = \lim_{t \to \infty} \varphi_1(t)^{-1} = 2$ and λ_2, respectively.

4. SIMULATION RESULTS

4.1 Funnel control performance with relative degree one

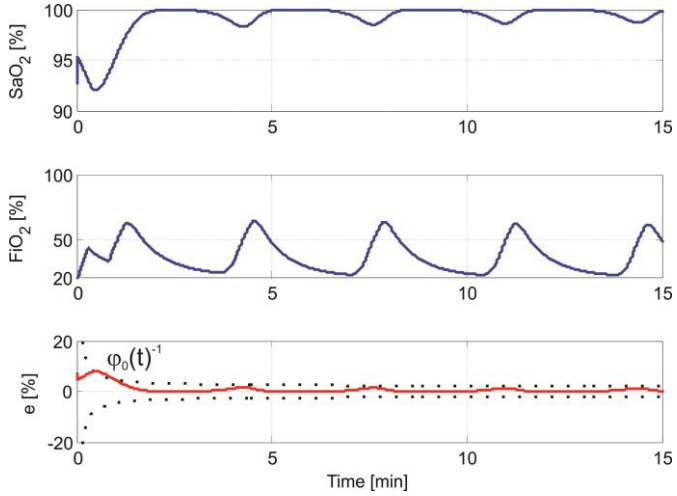

Fig. 6. Dynamical response of funnel control with relative degree one using hyperbolic funnel boundary.

The simulation of funnel controller with relative degree one is shown in Fig. 6 using hyperpolic function as given in section 3.1. The response of the cardiopulmonary system is based on a given low tidal volume of V_T = 125 ml, simulating of one lung ventilation for 15 min. To keep the oxygenation in a high level, SaO_{2ref} = 99.9% is set for the reference tracking objective. At the beginning, SaO_2 starts to decrease from 95% to 93%, reflecting hypoxia. Simultaneously, the funnel controller acts to maintain the control objective of SaO_{2ref} = 99.9% by increasing FiO_2 up to 60%. e(t) lie inside the prescribed hyperbolic funnel boundary $\varphi_0(t)^{-1}$.

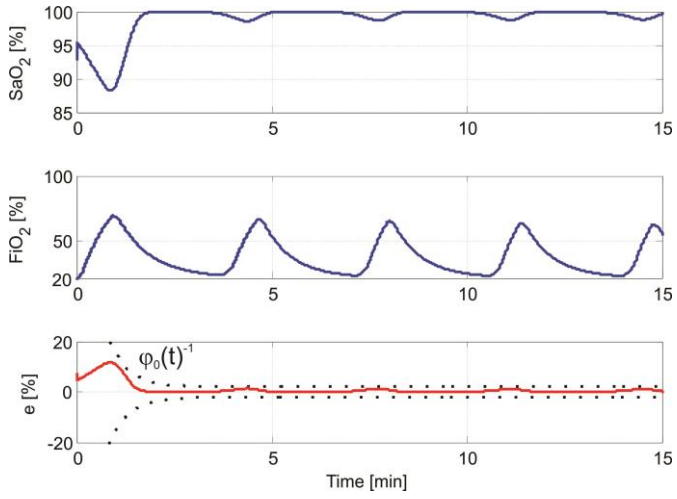

Fig. 7. Dynamical response of funnel control with relative degree one using exponential funnel boundary.

The control performance using exponential boundary also gives an acceptable result to control SaO_2, shown in Fig. 7. With this alternative, we can see that the transient response is slightly worse than hyperbolic funnel boundary as SaO_2 is below 90% at the early time of funnel control.

4.2 *Funnel control performance with relative degree two*

The resulting funnel controller as described in section 3.2 with relative degree of two was tested for its control performance for the cardiopulmonary system of Fig. 1 with low V_T. Figure 8 shows the performance of designed funnel controller under hypoxia where V_T = 125 ml, simulating one lung ventilation for time < 15 min and V_T = 75 ml, simulating an extreme atelectasis condition for time ≥ 15 min. Again, SaO_{2ref} = 99.9% is set for the reference tracking. At the beginning, SaO_2 starts to decrease from 95% to 92%, reflecting hypoxia and the funnel controller acts to maintain the control objective of SaO_{2ref} = 99.9% by increasing FiO_2 up to 80% and gradually reducing its peak cycle to 60% as shown in Fig. 8.

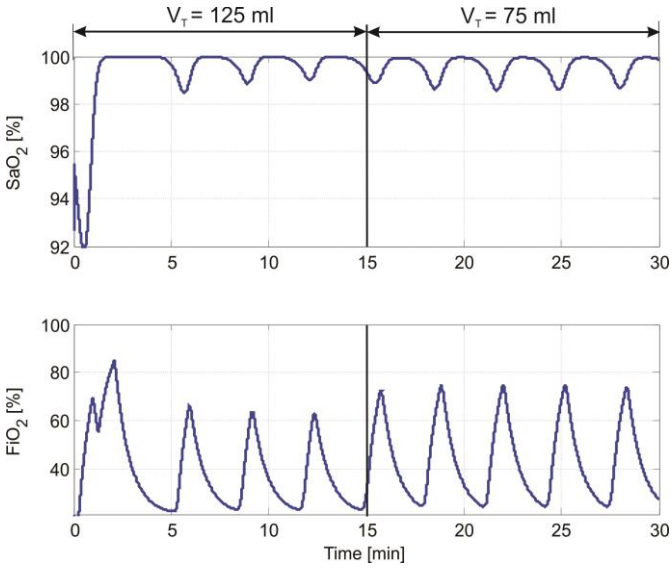

Fig. 8. Funnel control performance under hypoxia with an abrupt change of reduced tidal volume at time = 15 min.

Once an abrupt change from V_T = 125 ml to V_T = 75 ml is introduced to the cardiopulmonary at time > 15 min, the controller performs well to maintain its control objective by rising up the peak of FiO_2 to almost 80%. Based on the simulation, the funnel controller should be able to regulate SaO_2 for the extreme condition of atelectasis. In addition, Fig. 9 shows the evolution of e(t) and $\dot{e}(t)$ inside the prescribed hyperbolic funnel boundaries.

5. DISCUSSION

Due to a non-uniform distribution of blood flow into different tissues, the cardiopulmonary model used for this simulation is composed of three main compartments: lung, body and brain. Under hypoxia, Q_B and Q_T increase to compensate the poor arterial oxygen saturation (SaO_2) based on eq. (1), which reflects the mechanism to cope with impaired oxygenation. In addition, the model can represent a reduction of SaO_2 if V_T decreases during mechanical ventilation, simulating existing atelectatic region. The simulation results

of the model with FiO_2 = 9% give similar results from the literature (Fincham and Tehrani, 1983a). We therefore assume that the mathematical description of this model is valid for our purpose of SaO_2 control and there is no measurement dynamics or measurement error in the study.

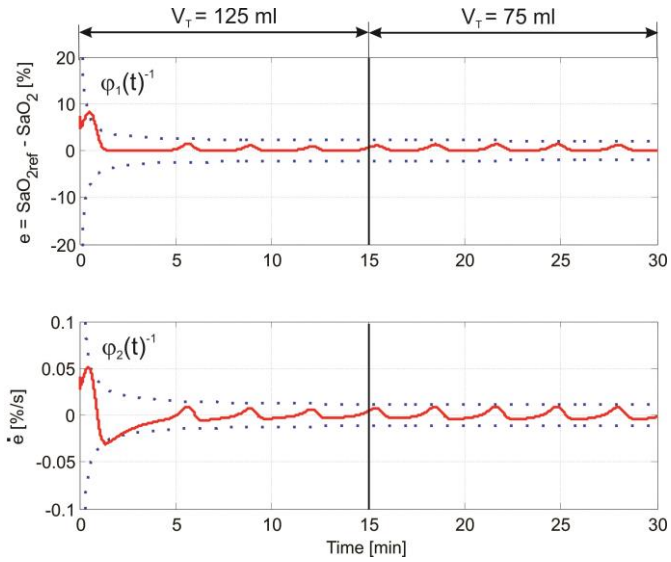

Fig. 9. Error evolution within a designed hyperbolic funnel boundary for a control of SaO_2 using oxygen therapy.

The proposed funnel control of relative degree one and two could satisfy the control objective with an allowable error margin as determined by λ value. However, the controller with relative degree two offers one more degree of freedom to control $\dot{e}(t)$ or force it within the predefined funnel boundary. The great advantage of this controller is to save time for identification under critical situation, to generate the optimal FiO_2 input for the patient with hypoxia and to avoid hyperoxia that may cause from the treatment. In our application, the perfect tracking performance is not required and this relieves further requirements of control design, for example additional filter design or tuning extended PI controller, which was implemented for speed and position control of servo-system (Hackl *et al*., 2011).

Our future work will be to implement this control algorithm in order to stabilize and to regulate SaO_2 for mechanically ventilated patient using patient-in-the-loop configuration. From the application perspective, the control strategy may be applied to various clinical scenarios, for example home-based ventilation for senior citizen or for patients with apnea, intensive care unit or anesthesia, which should offer a generalized solution for all patients with no need for individual system identification.

6. CONCLUSION

In this article, two funnel controllers based on vertical distance are proposed to control the complex cardiopulmonary system with possible pathophysiological change of atelectasis. A poor oxygenation can be observed from the simulation if air (FiO_2 =0.21) is only given to the subject of low V_T. Oxygen therapy is therefore required to keep SaO_2 in a high level (> 95%). The controllers of relative degree one and two show good performance to maintain this control objective by tolerating an error bound including an optimal therapy in avoiding hyperoxia. Based on the simulation result, the designed controllers should provide a practical solution for the control of oxygenation for the plant with nonlinear, time-delay and possible various uncertain factors using this non-identifier based approach. This concept should subsequently be evaluated in real applications.

REFERENCES

Bullinger E. and Allgöwer F. (2005). Adaptive λ-tracking for nonlinear higher relative degree systems. *Automatica*, 41, 1191-2000.

Clark J. M. (1974). The toxicity of oxygen. *American Review of Respiratory Disease*, 110 (6 Pt 2), 40–50.

Claure N. and Bancalari E. (2013). Automated closed loop control of inspired oxygen concentration. *Respiratory Care*, 58 (1), 151-161.

Defares J.G., Derksen H.E. and Duyff J.W. (1960). Cerebral blood flow in the regulation of respiration. *Acta. Physiol. Pharmacol. Neerlandica*, 9, 327-360.

Fincham W.F. and Tehrani F.T. (1983a). A mathematical model of the human respiratory system. *J. Biomed. Eng.*, 5, 125-133.

Fincham W.F. and Tehrani F.T. (1983b). On the regulation of cardiac output and cerebral blood flow. *J. Biomed. Eng.*, 5, 73-75.

Hackl C.M., Ji Y. and Schröder D. (2007). Enhanced funnel-control with improved performance. *16th Mediterranean Conference on Control and Automation*, T01-016, 1-6.

Hackl C.M., Hopfe N., Ilchmann A., Mueller M. and Trenn S. (2013). Funnel control for systems with relative degree two. *SIAM J. Control Optim*., 51(2), 965-995.

Hackl C.M., Hofmann A.G. and Kennel R.M. (2011). Funnel control in mechatronics: an overview. *50th IEEE Conference on Decision and Control and European Control Conference*, 8000-8007.

Ilchmann A. and Mueller M. (2009a). Robustness of funnel control in the gap metric. *SIAM J. of Control and Optimization*, 58(5), 3169-3190.

Ilchmann A. and Mueller M. (2009b). Robustness of λ-tracking and funnel control in the gap metric. *IEEE CDC and CCC*, 85-90.

Ilchmann A., Ryan E.P. and Sangwin C.J. (2002). Tracking with prescribed transient behavior. *ESIAM: Control, Optimisation and Calculus of Variations*, 7, 471-493.

Ilchmann A., Ryan E.P. and Trenn S. (2004). Adaptive tracking within prescribed funnels. *Proceedings of the 2004 IEEE International Conference on Control Applications*, 2, 1032-1036.

Mandaloju N.P. and Trenn S. (2006). Analogue implementation of the funnel controller. *PAMM Proc. Appl. Math. Mech*., 6, 823-824.

Pierson D.J. (2013). Oxygen in respiratory care: a personal perspective from 40 years in the field. *Respiratory Care*, 58 (1), 196-204.

Zambon M. and Vincent J.L. (2008). Mortality rates for patients with acute lung injury/ARDS have decreased over time. *Chest*, 133 (5), 1120-1127.